F20: Magneto Optic Trap

Martin Horbanski, Jan Krieger
tutor: Dr. Alois Mair

June 11, 2005

Abstract

This report describes the result of our lab course about the magneto optic trap (MOT). We first describe the theory of this experiment and then explain the experimental setup as well as the results that we obtained. We were able to record a high resolution spectrum of the rubidium D2-line, that was used to cool down and trap rubidium atoms (^{85}Rb). We then characterized our MOT, were able to optimize the number of trapped atoms and measured the dependence of the number of trapped atoms and the loading rate on external parameters. Finally we will discuss different models for the trap that allow us to estimate the temperature of the atomic cloud, including a simulational approach.

Contents

1 Cooling the Atoms

Cooling atoms means that we want to decrease the momentum of the atoms. This requires a velocity dependent dissipative force.

If an atom absorbs a photon it will change its momentum by $\Delta\vec{p} = \hbar\vec{k}$. Now the atom can relax either by stimulated or by spontaneous emission of a photon.In case of stimulated emission, the atom emits a photon with $\vec{k}_{re} = \vec{k}_{laser}$ which has the same direction as the photon from the laser field and therefore the overall momentum transfer to the atom is zero. In case of spontaneous emission the photons are reemited isotropic and the mean value of the momentum of the reemited photon $< p_{re} >$ is zero. This results in an overall momentum transfer to the atom $\vec{p}_{eff} = \hbar\vec{k}$.

Since we want to cool the atoms we have to make sure that only those atoms that are propagating in the opposite direction of the laser beam absorb photons. This can be done by using the Doppler effect. For an atom which is moving towards the laser-beam the photons are blue detuned, and in the other case red detuned. Assume that a still atom is resonant on a certain frequency ω_{res}. If you red detune the laser to $\omega_{laser} = \omega_{res} + \delta$, then atoms which are moving towards the laser with $\vec{v}_{atom} \cdot \vec{k}_{laser} = \delta$ will be resonant. The resulting force which acts on an atom can be written as:

$$\vec{F}(\vec{v}) = \hbar\vec{k}\frac{\Gamma}{2}\frac{I/I_0}{1 + I/I_0 + \left(\frac{2(\delta - \vec{k}\vec{v})}{\Gamma}\right)^2} \tag{1}$$

I, laser intensity; I_0, saturation intensity
$\delta = \omega_{laser} - \omega_{res}$, detuning of the laser
$\vec{k}$, the wave vector;
Γ, decay rate of the exited state

If we plug $v = 0$ in (1) we see that the force on zero-velocity atoms is not zero. To compensate this we use three orthogonal pairs of counter propagating laser beams (with red detuning $\delta < 0$), which is also known as an *optical melasse*. For the sake of simplicity we will only discuss the onedimensional case. For small laser intensities ($I/I_0 << 1$) we get with equation (1):

$$F(v) = \hbar k\frac{\Gamma}{2}\left(\frac{I/I_0}{1 + I/I_0 + \left(\frac{2(\delta - kv)}{\Gamma}\right)^2} - \frac{I/I_0}{1 + I/I_0 + \left(\frac{2(\delta + kv)}{\Gamma}\right)^2}\right) \tag{2}$$

$$\underset{I/I_0<<1}{=} \hbar k\frac{\Gamma}{2}\left(\frac{I/I_0}{1 + \left(\frac{2(\delta - kv)}{\Gamma}\right)^2} - \frac{I/I_0}{1 + \left(\frac{2(\delta + kv)}{\Gamma}\right)^2}\right) \tag{3}$$

If we do a Taylor expansion of $F(v)$ around $v = 0$ we get:

$$F(v) = 0 \cdot v^0 + \frac{8\hbar k^2\delta\frac{1}{\Gamma}\frac{I}{I_0}}{\left(1 + \frac{4\delta^2}{\Gamma^2}\right)^2} \cdot v + 0 \cdot v^2 + O(v^3) \underset{\delta<0}{\simeq} -\alpha v \tag{4}$$

According to this model the velocity would decrease exponentially to zero. But this model does not include the discrete absorption and emission process. If we take this into account we get the *Doppler limit* (the lowest temperature reachable):

$$T_{Doppler} = \frac{\hbar\Gamma}{2k_B} \tag{5}$$

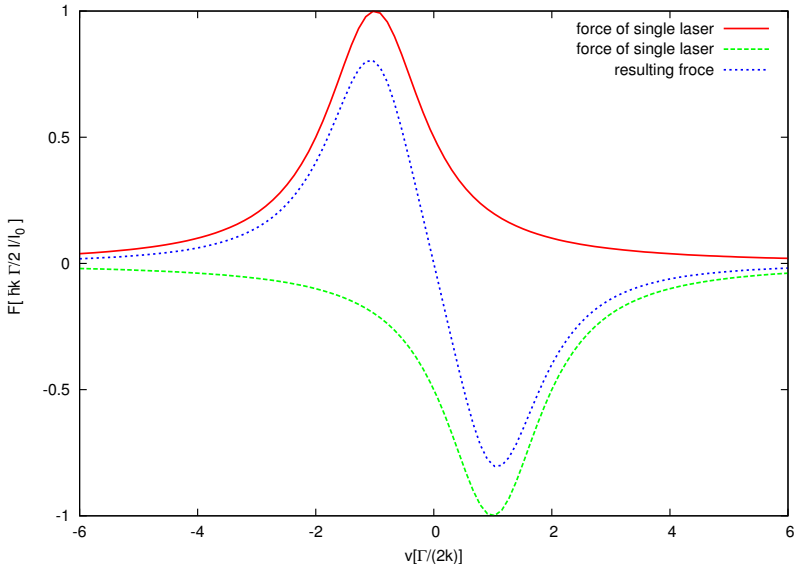

Figure 1: Light force depending on atom's velocity for $\delta = -\frac{\Gamma}{2}$

2 Trapping the Atoms

According to the optical Earnshaw theorem [Phillips 1992, p. 321] the optical melasse does not implement a trap. Even if they are in the cross-over point of the laser beam, the atoms will diffuse out of the cooling area. Therefore we need an additional restoring force which depends on the atom's position. One possible solution is the magneto optical trap (MOT). To keep things simple we will consider a two level system with a transition ($F = 0 \rightarrow F = 1$). Additionally we introduce a 1-dim. linear magnetic field (along the z axis) with $B = 0$ at $z = 0$. Due to the Zeeman effect we get a energy splitting of the three degenerated energy levels of the F=1 state, which depends on the atom's position (see fig. 2).

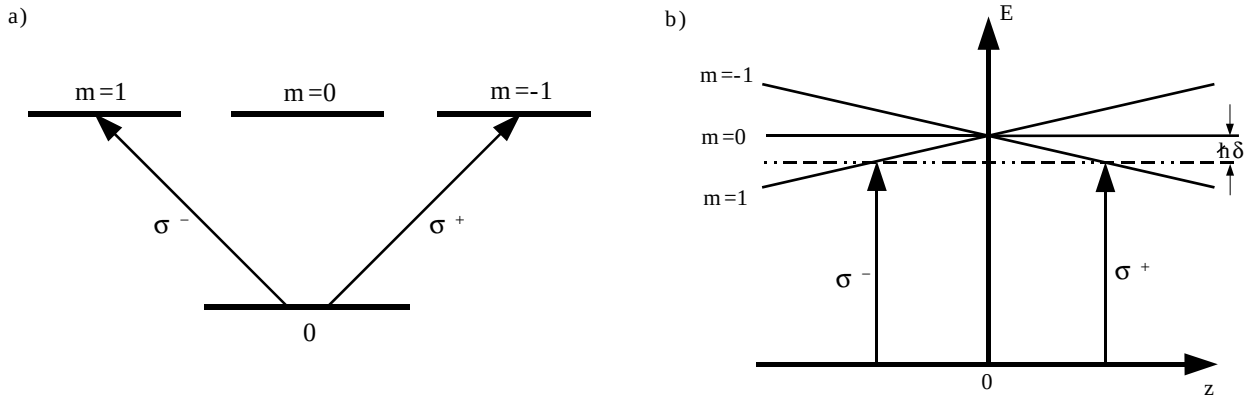

Figure 2: a) Transition scheme; b) Energy levels in the spatially varying filed; the dashed line is the energy of the laser-photons

Without loss of generality we can choose the magnetic field so that the $m = -1$ level is lowered for increasing z, and the other way around for $m = -1$. Now we add two counter propagating laser beams in z-direction. The beam which propagates in positive z-direction has a σ^+ helicity with respect to the atom and the other beam a σ^- helicity, this means that both beams have the same polarization (see fig. 3). The laser is detuned by δ from the resonance of the transition (fig. 2). Due to the Zeeman splitting and the red detuning of the laser the probability for a atom at $z < 0$ to absorb σ^+ photon is much higher than the probability to absorb a σ^- photon, and therefore the atom feels a force which brings it back to $z = 0$. As

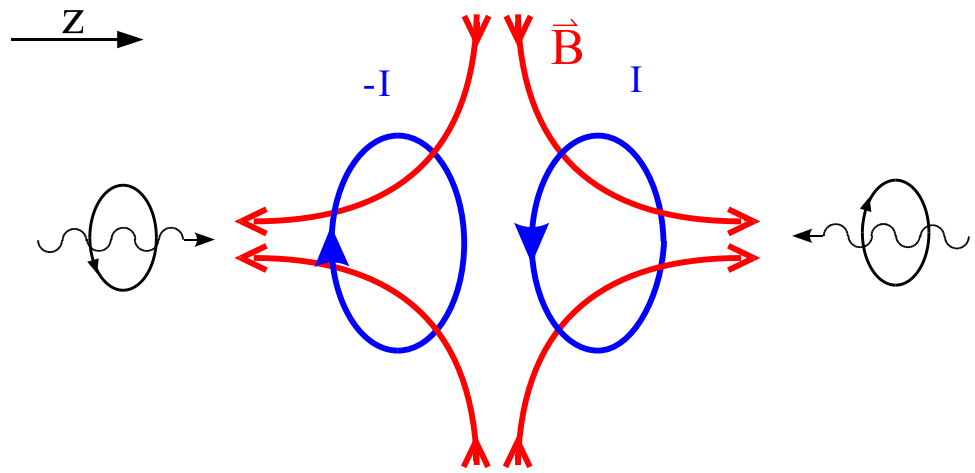

Figure 3: 1-dimensional MOT, $\sigma^{\pm}$ are helicities

total force on the atoms we get [Phillips 1992, p. 323]:

$$F(v,z) = F_{\sigma^+} + F_{\sigma^-} = \frac{\hbar k \Gamma}{2}\left(\frac{I/I_0}{1+4\left(\frac{\delta - kv - \beta z}{\Gamma}\right)^2} - \frac{I/I_0}{1+4\left(\frac{\delta + kv + \beta z}{\Gamma}\right)^2}\right) \tag{6}$$

In the limit of small v and z we get:

$$F(v,z) = \frac{2\hbar k (2I/I_0)(2\delta/\Gamma)[kv + \beta z]}{(1+(2\delta/\Gamma)^2)^2} \tag{7}$$

This can be written as:

$$\ddot{z} + \gamma \dot{z} + \omega_{trap}^2 z = 0 \tag{8}$$

which is the equation of a damped harmonic oscillator. This shows that we can cool (dissipative part) and trap (harmonic potential) the atoms.

3 The Rubidium Atoms

The natural occurrence of Rubidium (which is also found in the lab) is 72% of ^{85}Rb and 28% of ^{87}Rb. In our experiment we will use the $5s \leftrightarrow 5p$ transitions (D-line) of ^{85}Rb (see fig. 4). The transition which is used for cooling is $5S_{1/2}, F = 3 \leftrightarrow 5P_{3/2}, F = 4$. Since this is not a simple two level system, there is a small but existing probability for the transition form $5P_{3/2}, F = 4$ to $5S_{1/2}, F = 2$ (this happens in about 1 in 1000 cycles). If the atom is in the $5S_{1/2}, F = 2$ state (*dark state*), it does not interact with the *cooling laser* anymore. But since the transition rate for $5S_{1/2}, F = 3 \leftrightarrow 5P_{3/2}, F = 4$ is quite big, we would loose all atoms after a short period and a permanant trap would not be possible.

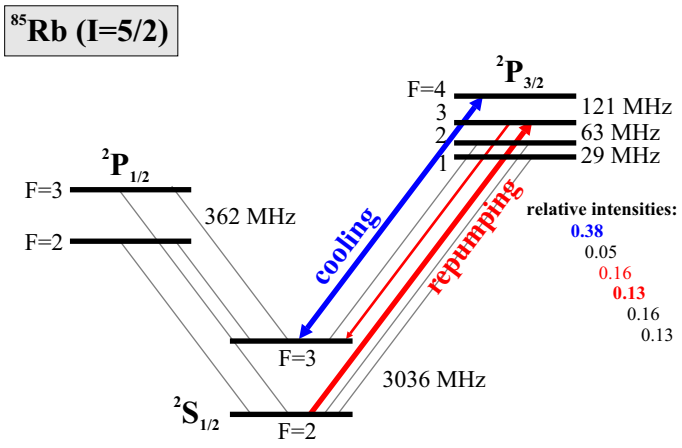

Figure 4: fine and hyperfine structure of the ^{85}Rb D-line [Mot 2004]

The solution is a second laser which pumps from $5S_{1/2}, F = 2$ to $5P_{3/2}, F = 3$. From there the atoms can get back to the $5P_{3/2}, F = 4$ state, which closes the cycle.

4 Doppler-free saturation spectroscopy

At room temperature the width of atomic resonances is dominated by the Doppler effect. The Doppler broadening of a spectral line can be calculated as [Haken 2000, p. 302]:

$$\Delta\omega_D = \frac{\omega_0}{c}\sqrt{\frac{8k_BT \cdot \ln 2}{m_0}} \tag{9}$$

For the ^{85}Rb D-Lines at room temperature we get ($\omega_0 = 2.41 \cdot 10^{15}s^{-1}$, $m_0 = 1.411 \cdot 10^{-25}kg$, $T = 300K$) $\Delta\omega_D = 3.247 \cdot 10^9 s^{-1}$. Comparing this to the natural linewidth $2\pi\Gamma \approx 3.8 \cdot 10^7 s^{-1}$ we see that the Doppler broadening at room temperature is two orders of magnitude bigger. To see single resonance peaks we have to limit spectroscopy to one velocity. This can be done by the method of **Doppler-free saturation spectroscopy**. For this setup we use two counterproparating laser-beams. A "pump beam" with a high intensity is transmitted through an atomic vapour cell, to pump the atoms into higher energy levels. From the opposite direction we sent a "probe beam" with exactly equal beam path and frequency, but with lower intensity ($\approx 1/10$ of the "pump beam"), and record its absorbtion in the atomic vapour cell (spectroscopy signal).

Now let's consider a simple two level system with a ground state $|g\rangle$ and an exited state $|e\rangle$ and a resonance frequency ω_0. If we shine in light with frequency ω_0 the pump beam will excite atoms with $v \simeq 0$ into state $|e\rangle$, while atoms with $v \neq 0$ will out of resonance due to the Doppler effect. Now the "probe beam" sees nearly no atoms in $|g\rangle$ and therefore it is only weakly absorbed. But if we red detune the laser frequency from ω_0 to $\omega = \omega_0 - \delta$, the "pump beam" will be in resonance with atoms that move towards it ($v > 0$) and the "probe beam" will address atoms with $v < 0$ which are not excited, and therefore it will be absorbed. Respectively for blue-detuned light. According to the above, we will get an intensity peak at the resonance frequency (lamb dip) (see fig.4) and therefore it is possible to gain a resolution which is not depending on the Doppler broadening of a spectral line.

The situation get's a little bit more complicated if we have multilevel atoms e.g. let's consider a system with one ground state $|g\rangle$ and two exited states $|e_1\rangle$ and $|e_2\rangle$, transition frequencies $\omega_1 = \omega(|g\rangle \to |e_1\rangle)$ and $\omega_2 = \omega(|g\rangle \to |e_2\rangle)$ with $\omega_1 < \omega_2$ and $\omega_2 - \omega_1$ smaller than the doppler broadening. Now if we detune our laser to $\tilde{\omega} = \frac{\omega_1+\omega_2}{2}$ then we will see an extra resonance peak between the two resonance peaks, the so called **cross over peak**. This can be understood if we consider atoms which are moving away form the "pump-beam" with $v < 0$ so that the "pump" is resonant with the ω_1 transition, but for the same atoms the "probe" is resonant with the ω_2 transition, because:

$$\omega_1 = \tilde{\omega} - kv \tag{10}$$

$$\Rightarrow kv = \tilde{\omega} - \omega_1 \tag{11}$$

and the same atoms see the probe with ω':

$$\omega' = \tilde{\omega} + kv \tag{12}$$

$$\underset{(11)}{\Rightarrow} \omega' = \tilde{\omega} + \tilde{\omega} - \omega_1 \tag{13}$$

$$\underset{\tilde{\omega}=(\omega_1+\omega_2)/2}{\Rightarrow} \omega' = \omega_2 \tag{14}$$

The "pump-beam" pumps nearly all atoms in the $|e_1\rangle$ state, but this leads to a reduction of the population density of the groud state $|g\rangle$, which makes the atoms "transparent" for the "probe-beam", and therfore we see a cross-over peak.

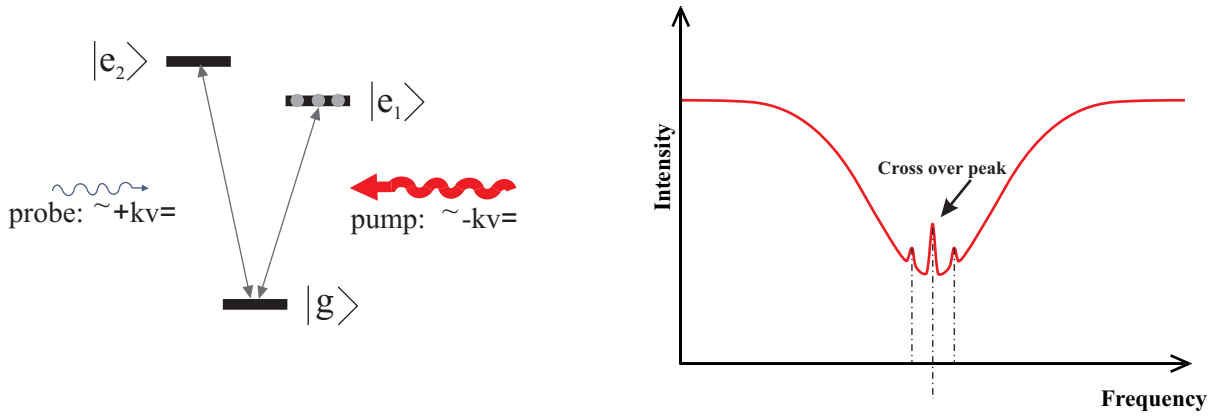

Figure 5: Absorbtion line with lamb dip.

5 Experimental Setup

In this chapter we will explain the experimental realisation of the theoretical concepts and the results obtained with this setup. There are two major parts in the experiments. First we took a spectrum of the rubidium (Rb) D2-line that is used to cool the atoms. Then we implemented a magneto optical trap (MOT). We then characterized our MOT and tried to find dependencies of its controllable parameters.

5.1 Lasers and Laser Lock

To implement a MOT you need lasers that are stabilised precisely to a specific frequency (accuracy $\approx$ some MHz), that has to be detunable. So we need lasers with tunable frequency, to make electronic stabilisation of the frequency possible.

In this lab we used two lasers, named COCO and ROY. ROY was used to cool the atoms down, i.e. to produce the three counter propagating beams (frequency: slightly detuned from $F = 3 \rightarrow 4$ line). COCO is used to repump the atoms from the dark ground state ($F = 2 \rightarrow 4$ line). Both have the same internal setup. They are diode lasers with a tunable external cavity. It is possible to tune the frequency of a diode laser, as these lasers do not emit a single line, but a narrow continuum of frequencies. Fig. 6 shows the basic setup of these lasers. They use a Littrow diffraction grating. In this configuration the first order is reflected back into the diode and the zeroth order can be used for the experiment. By changing the position of the grating (using a piezo element), it is possible to change the external cavity that is formed between the grating and the laser diode itself. This of course changes the wavelength of the laser. In

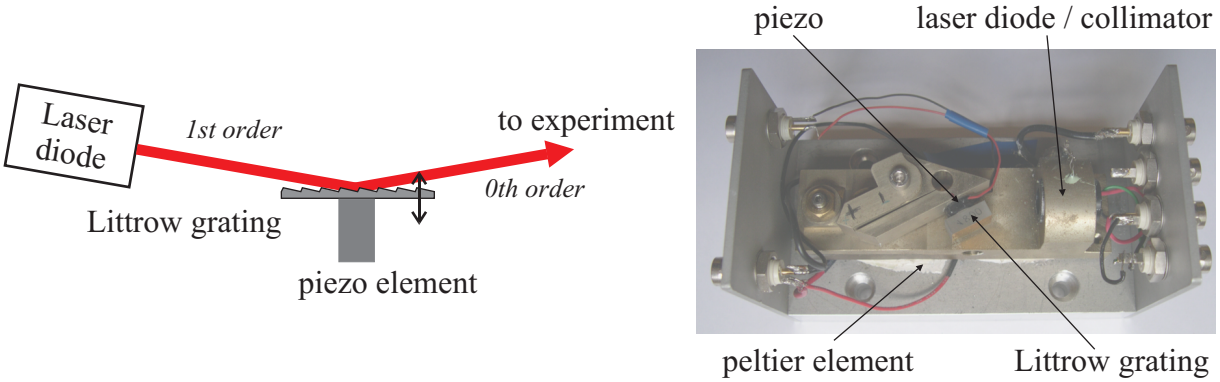

Figure 6: basic setup for a tunable diode laser with a Littrow grating (left); photograph of the laser (right)

addition it is essential to stabilise the temperature and the current through the laser diode, as these two factors also change the wavelength and output power of the diode laser. The first task is done by using a peltier element and a temperature dependent resistor (NTC). The latter one has to be done electronically.

As we have already seen, the lasers have to be locked to a specific hyperfine line within the Rb-D2 line. Here this is done by adding two spectroscopy setups to the lasers. We used Doppler-free saturation spectroscopy, that is described in 4 and 5.3. From these, an error signal that reflects the detuning from the spectral line has to be derived. The derivative of the spectroscopy signal is a good choice, as it shows a zero crossing if the laser frequency passes a peak. So we can use PI-regulators to stabilize the frequency of the lasers.

The stabilisation appeared to be quite resistant to disturbance. This is especially true for ROY. We lost laser lock only once or twice a day, while COCO lost its lock in about every hour. By clapping in the hands we could disturb the lasers i.e. they were forcibly detuned. Both lasers returned reliably to their lock positions.

Fig. 7 shows the complete optical setup in the lab. The two linearly polarised laser beams (cooler and repumper) are combined in a beam splitter. The resultant beam is widened, using a telescope. Two half-waveplates and two polarising beam splitters are used to create three linearly polarised laser beams with changeable intensity. They are then circularly polarized and sent into the vacuum chamber, where they cross to form the MOT. All three beams have to have in about the same intensity, which can be varied by turning the half waveplates.

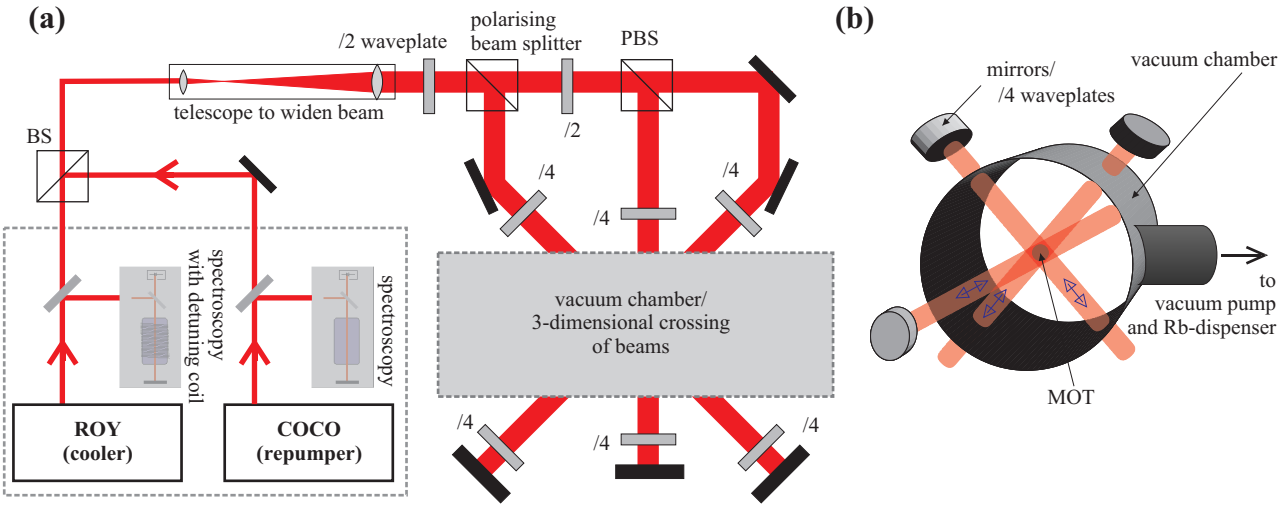

Figure 7: (a) complete optical setup, including vacuum chamber and spectroscopy (b) setup of the vacuum chamber

The polarisation of the beams leaving the vacuum chamber is changed to linear again, before they are reflected and sent back. With this setup the circular polarisation does not change, i.e. if the beam has σ^+ polarisation, the counter propagating also has σ^+ polarisation. This leads to $\sigma^{\pm}$-helicity of the beams, as mentioned before.

5.2 Mechanical Setup and Vacuum

The MOT itself is formed within a vacuum chamber that is kept at approximately $5 \cdot 10^{-9}$ mbar. The chamber is equipped with several glass windows that are used for the laser beams and to observe the MOT. There are also Rb-dispensers. The pressure is kept low by continuous pumping.

The two Helmholtz coils (actually they are in anti-Helmholtz configuration) are placed outside the vacuum chamber and attached to a constant current supply.

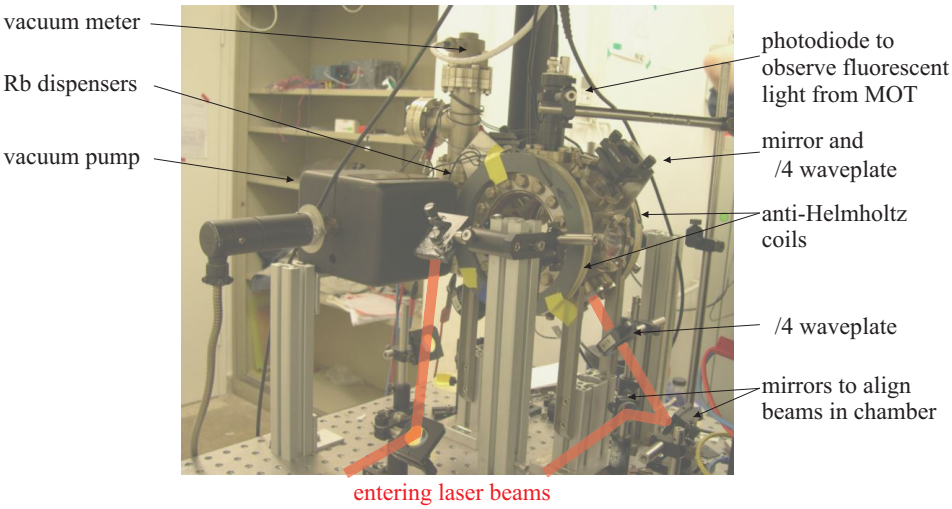

Figure 8: photograph of the experimental setup showing the vacuum chamber and optical elements for the laser beams

There is a small CCD-camera which is sensitive in the near IR spectrum and can therefore be used to image the trapped atom directly, as they show fluorescence while the laser is resonant to their D2-line. We were also able to record some small videos of the experiment, using this camera. Additionally the setup contains a photodiode with a precision current-to-voltage converter/amplifier which allowed us to measure precisely the power that is emitted over fluorescence by the atoms in the trap.

5.3 Spectroscopy Setup

Fig.9 shows the experimental setup for the Doppler-free saturation spectroscopy that is explained in 4. A small fraction of the laser light coming from COCO or ROY (pump beam) is sent through a gass cell that contains Rb vapour. The cell is heated to increase the vapour pressure. Behind the cell there is a mirror that reflects the beam back (probe beam). Then the beam is split again and sent to two photodiodes. One is a standard version that records the spectroscopy signal. The second one is an avalanche photodiode with acompanying electronics that generates a signal that is proportional to the derivative of the spectroscopy signal itself.

For the cooling laser there is also a detuning coil and a $\lambda/4$-waveplate. This allows us to change the position of the spectral lines of the Rb atoms due to the Zeeman effect. This is needed to allow a laser lock on a shifted spectral line, as it is needed for our experiment.

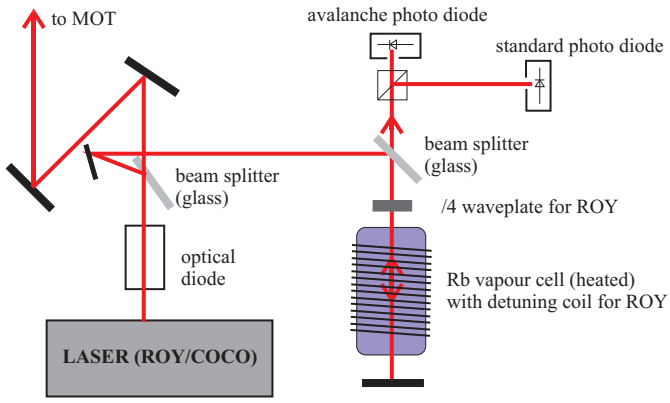

Figure 9: experimental setup for the Doppler-free saturation spectroscopy

6 Experimental Results

6.1 Rb-spectroscopy

We scanned over the complete D_2 line of ^{85}Rb and ^{87}Rb (see fig. 18 for the theoretical spectrum) using the laser named ROY, which is used to cool the atoms in the MOT.

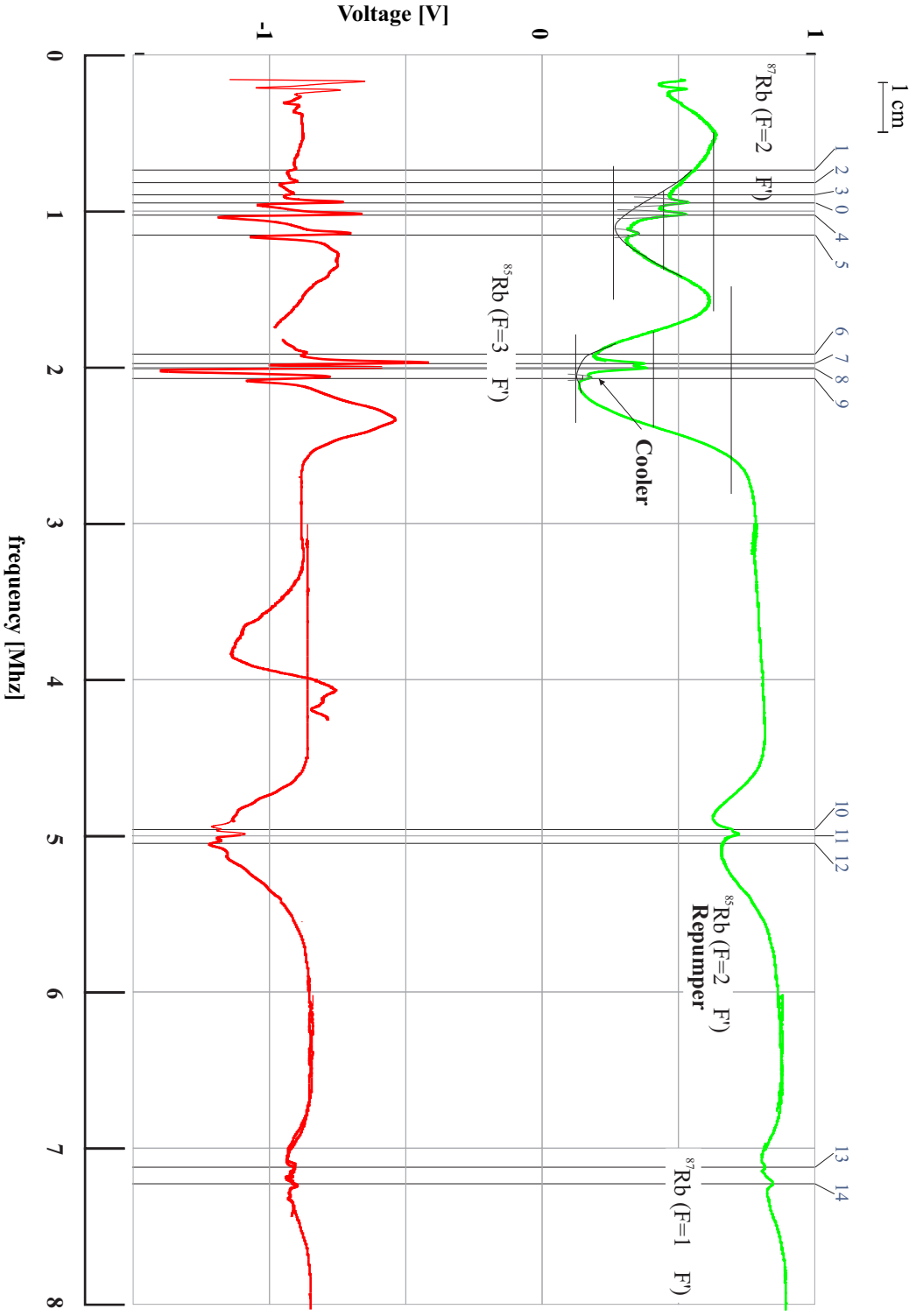

Figure 10: Rb-spectrum, taken with COCO. The upper (red) curve shows the spectroscopy signal. The lower (green) curve shows its derivative. The blue numbers mark the single lines. The lines for the cooling and the repumping laser of the MOT are marked also.

As it is impossible to tune the laser over the complete frequency interval, needed to record the complete line structure, we took several smaller scans that had to be combined to show the complete spectrum. Fig 10 shows our results. A complete scan is not possible, as the laser produces mode-jumps, i.e. new modes start to appear in the laser-cavity, that do not have the desired frequency. Some of the lines may be seen as peaks in the spectroscopy signal itself. But as one can see from our results there are more lines that can be found in the derivative of this signal. The position of the lines is slightly shifted to the right, when we compare the spectroscopy signal and its derivative. This may be explained by a retardation in the measurement electronics. The lines in fig. 10 are plotted according to the derivative.

The spectrum in fig. 10 shows both, the normal lines and the cross-over peaks that are created by our spectroscopy-method (see 4). To transform a line's position (measured in mm) into a frequency, we calculated a calibration factor α, using the known distance $\Delta\nu = 78.47\text{MHz}$ between the two big cross-over peaks of the ${}^{87}Rb(F = 2 \to F')$ group of lines (see fig18). From fig. 10 one gets a factor of:

$$\alpha = \frac{78.47\,\text{MHz}}{(2.5 \pm 0.8)\,\text{mm}} = (31.4 \pm 8.8)\,\frac{\text{MHz}}{\text{mm}}$$

The error is quite large, which depicts the uncertainty in adding the single scans together. Using this factor we could determine relative distances for all the lines within the ${}^{85}Rb$ and ${}^{87}Rb$ spectrum. When measuring the distances in fig. 10, we estimated an error of about 0.7 mm in their position, which is mainly given by the finite frequency resolution. Our results are shown and compared to the theoretical expectation in tab. 1 and 2. The spectrum shows a slow rise from left to the right. This can be explained by an increase in laser power while detuning the resonator. All measure lines are as expected theoretically within 1σ.

♯	**dist. to 0** [mm]	**dist. to 0** [MHz]	**line group**	**line**	**theoretical distance** [MHz]
1	(6.6 ± 1.0)	(207 ± 66)	${}^{87}Rb(F = 2 \to F')$	$F' = 1$	211.8
2	(4.1 ± 1.0)	(128 ± 47)		1→2 co	133.33
3	(1.6 ± 1.0)	(50 ± 34)		$F' = 2$	54.85
4	(2.5 ± 0.8)	78.47 (exact)		2→3 co	—
5	(6.5 ± 1.0)	(204 ± 65)		$F' = 3$	211.8
13	(194.2 ± 1.0)	(6097 ± 1709)	${}^{87}Rb(F = 1 \to F')$		distance of this group of lines
14	(197.5 ± 1.0)	(6201 ± 1738)			is about 6834.682 MHz

Table 1: The spectral lines measured in the ^{87}Rb-spectrum. The distances give the frequency distance to the line marked as 0. The theoretical data is taken from [Steck 2005]. 'co' stands for crossover line.

♯	**dist. to 9** [mm]	**dist. to 9** [MHz]	**line group**	**line**	**theoretical distance** [MHz]
6	(4.9 ± 1.0)	(168 ± 55)	${}^{85}Rb(F = 3 \to F')$	$3 \to 2$ co	152.5
7	(3.0 ± 1.0)	(103 ± 43)		$4 \to 2$ co	92
8	(1.9 ± 1.0)	(65 ± 38)		$4 \to 3$ co	60.5
9	0	0		$F' = 4$	—
10	(90.9 ± 1.0)	(3126 ± 800)	${}^{85}Rb(F = 2 \to F')$		distance of this group of lines
11	(92.1 ± 1.0)	(3168 ± 811)			is about 3036 MHz
12	(93.7 ± 1.0)	(3223 ± 825)			

Table 2: The spectral lines measured in the ^{85}Rb-spectrum. The distances give the frequency distance to the line marked as 9. The theoretical data is taken from [Kemmann 2001]. 'co' stands for crossover line.

We could also extract the line widths (FWHM) from fig. 10. First we measure the Doppler-broadened line widths (see tab. 3). From these one gets an estimate for the temperature

of the Rb-vapour in the spectroscopy cell. From theoretical considerations one gets for the Doppler-broadening $\Delta\omega_D$:

$$\Delta\omega_D = \frac{\omega}{c}\sqrt{\frac{8k_BT\cdot\ln 2}{m}} \qquad \Rightarrow \qquad T = \frac{m\cdot(\lambda_{D2}\cdot\Delta\nu_D)^2}{8k_B\cdot\ln 2} \tag{15}$$

With (15) we calculated the temperature of the Rb-vapour. The results are shown in tab. 3. With this method we measured a temperature of about (400 ± 140) K. This can be explained, as the rubidium cell is being heated to raise the rubidium vapour pressure in it.

(a)

line	**width $\Delta\nu_D$ [MHz]**	**Temperature T [K]**
^{87}Rb($F = 2 \to F'$)	(587 ± 139)	(395 ± 132)
^{85}Rb($F = 3 \to F'$)	(606 ± 172)	(411 ± 165)

(b)

line	**width** [MHz]
0	(41 ± 22)
4	(45 ± 23)
5	(48 ± 23)
9	(27 ± 20)

Table 3: Doppler-broadened (a) and Doppler-free (b) line widths and the temperature of the Rb-vapour, that was derived from them.

We could also estimate the Doppler-free width for some lines. The results are also shown in tab. 3. The natural line width would be (Γ_{D2} is the decay rate of the excited Rb-D_2 state):

$$\Delta\nu = \frac{\Gamma_{\mathrm{D2}}}{2\pi} \approx 6\,\mathrm{MHz} \tag{16}$$

The measured lines are still broader than the theoretical minimum width, but they are about one order of magnitude smaller than the Doppler-broadened spectral lines.

6.2 Implementing the MOT and Basic Characterisation

6.2.1 Implementing the MOT

The next task in the lab course was to implement the magneto-optical trap itself. To do this we had to align the beams within the chamber in a way that maximizes then overlap region. In this region the MOT will form. This task did not cause severe problems, so we could establish the trap on the first of three days in the lab. The alignment of the $\lambda/4$ waveplates is not critical either. The light just has to be in about circularly polarized a slight elliptical polarization does not show any large effect.

On the second day we could further optimize our settings, by measuring the fluorescent light from the trapped atoms and aligning the setup accordingly. Fig. 11 shows some photographs of our MOT. You can recognize the three laser beams and the bright (white) atomic cloud in the region where they cross.

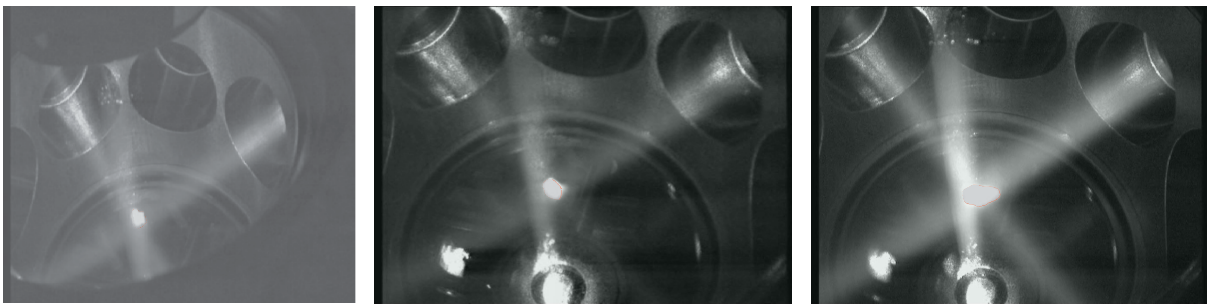

Figure 11: Pictures of atoms in our MOT, taken using a CCD camera. The red lines mark the atomic cloud.

6.2.2 Number of Atoms

To measure the fluorescent light we used the photodiode, mentioned in 5.2. As the size of this photodiode, its spectral response and distance to the trapped atoms is known we could calculate the overall power of the emitted fluorescence light, which enables us to measure the number of atoms in the trap. To estimate the number of atoms, we assumed that one photon of energy $h\nu_{\mathrm{D2}} = \frac{hc}{\lambda_{\mathrm{D2}}}$ is emitted every lifetime $\tau = \frac{2\pi}{\Gamma_{\mathrm{D2}}}$ of the excited Rb-state by half of the atoms (number of atoms: N, at the maximum, $N/2$ atoms are in the excited state). This gives us:

$$N = \frac{P_{\mathrm{detected}} \cdot \tau}{h\nu} \cdot \frac{2 \cdot r_{app}^2}{r_{\mathrm{detector}}^2} \tag{17}$$

where $r_{app} = (10 \pm 2)$ cm is the distance between the trapped atoms and the photodiode and $r_{\mathrm{detector}} = (3.5 \pm 1)$ mm is the radius of the circular photodiode. The factor $\frac{4 \cdot r_{app}^2}{r_{\mathrm{detector}}^2}$ calculates the fraction of light that is emitted into the photodiode. Using (17) we calculated that our trap contained a maximum of about 10^6 atoms.

It does not make sense to estimate the error using Gaussian error propagation, as we do not have good estimates for the errors of our measured variables. We believe the error is at least about 30%. This is the relative error that is obtained soleily from the uncertainty in the geometric factor $\frac{4 \cdot r_{app}^2}{r_{\mathrm{detector}}^2}$.

With (17) we estimated about $5 \cdot 10^5$ trapped atoms.

6.3 Loading Rate Measurement

To model the loading behaviour of the trap we assumed that it has a constant loading rate γ and a loss that is proportional to the number of atoms $-\beta \cdot N$ (see [Stuhler 2001]). This gives a differential equation:

$$\frac{dN}{dt} = \gamma - \beta \cdot N \tag{18}$$

The solution of this equation is simply

$$N(t) = N_0 \cdot (1 - e^{-t/\tau}), \qquad \text{with} \qquad \tau = \frac{1}{\beta} \tag{19}$$

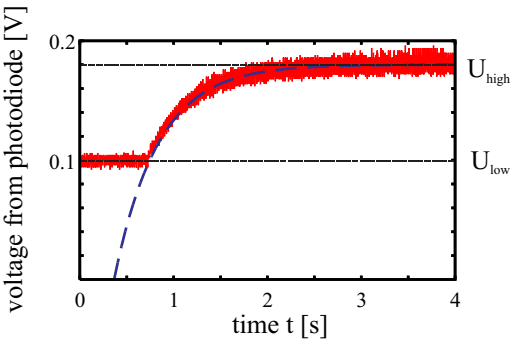

Figure 12: example recording from loading rate measurement

which means that $N(t)$ approaches a global maximum, where the flows to and from the trap are equal ($t \gg 0 \quad \Rightarrow \quad \gamma = \beta$). The constant loading rate is then:

$$\gamma = N_0 \cdot \beta = \frac{N_0}{\tau} \tag{20}$$

To actually measure τ, we recorded the fluorescent light while the trap was loading up. This gave us curves, as the one shown in fig. 12. We used GnuPlot to fit a function, like (19) to the data. From this fit we took τ. We could also determine the background intensity (proportional to U_{low}) with no lasers on, i.e. no fluorescence and the intensity, when the trap is full. From the latter one we could calculate the number of atoms in the trap (see equation (17)).

There are several parameters in this experiment that can influence the loading rate as well as the number of atoms. We picked out two of them. We choose the Detuning of the cooling laser (ROY) and the magnetic field, i.e. the current through the Helmholtz coils ($I \propto B$), as these seemed crucial and are relatively easy to measure.

The results, obtained when varying the magnetic field are shown in fig.13. The number of atoms seems to increase linearly with the magnetic field. The same seems to be true for

the loading rate γ. The loss rate β seems to reach a constant level for high magnetic fields. These results can be understood if we take into account that the strength of the magnetic field determines the height $\Phi_{\max}$ of the trap potential. Atoms may be trapped if their energy $E_{\text{kin}} = p^2/2m$ is below the trap potential, i.e. a raising magnetic field increases the fraction of atoms that may be trapped.

Atoms may always leave the trap, if they get an additional impulse from external hot atoms. If the magnetic field and therefore $\Phi_{\max}$ increases, it is getting more and more unlikely that an atom's kinetic energy after a stroke is big enough to cross $\Phi_{\max}$. This explains the decrease of the loss rate β. There is a constant bias, that the loss rate decreases to. This could be explained by higher order effects, like strokes between excited atoms. A second explanation could be a decreased cooling rate in the center of the trap (that gets smaller for higher magnetic fields) as the atomic cloud has a non-vanishing optical density.

The errors of N (number of atoms) is assumed as 30% (see 6.2.2). The errors of β and γ result from gaussian error propagation. The error of τ, was taken from GnuPlot.

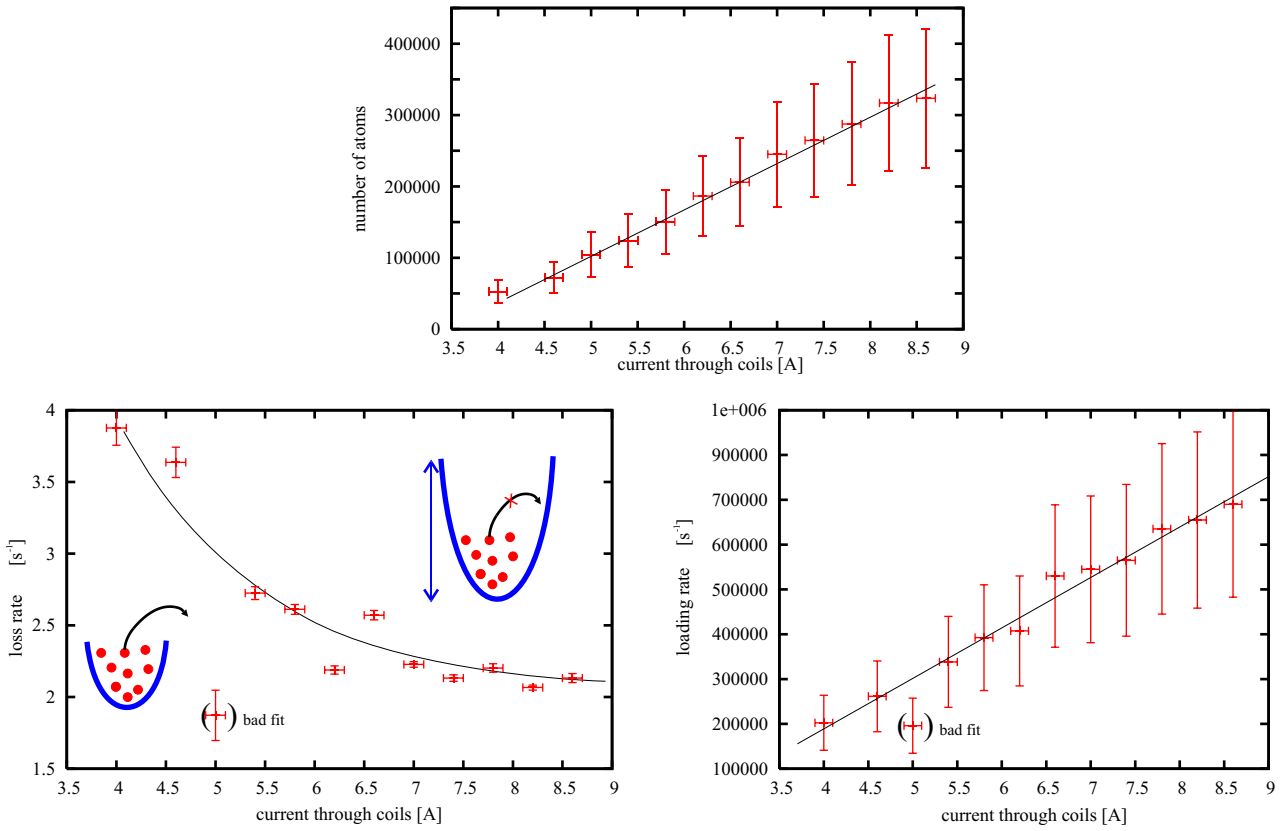

Figure 13: number of atoms N, loading rate γ and loss rate β versus current through the pair of Helmholtz coils

We also measured the loading rate in dependence of the detuning $\Delta\nu$ of the cooling laser. The detuning is created by a coil around the spectroscopy cell, that is fed by a constant current I (see 5.3). As the coil does not get hot its resistance is constant and therefore it is sufficient to measure the voltage applied to the coil. We do know that the detuning is proportional to the magnetic field which is proportional to the current I. Therefore it is easy to stretch the x-axis from voltage to detuning by a linear factor. Fig.14 shows our results.

In fig.14 one can clearly see that there is a domain where the biggest number of atoms is beeing trapped. Of course this is also reflected in the loss and loading rates. For the errors we used the same estimates as before. This result can also be understood quite simply: If the detuning is low or high the laser is resonant on too cold or too hot atoms with respect to their

distribution in temperature. So we should get a maximum number of atoms when the detuning is optimal with respect to the atoms in the chamber (see fig. 14).

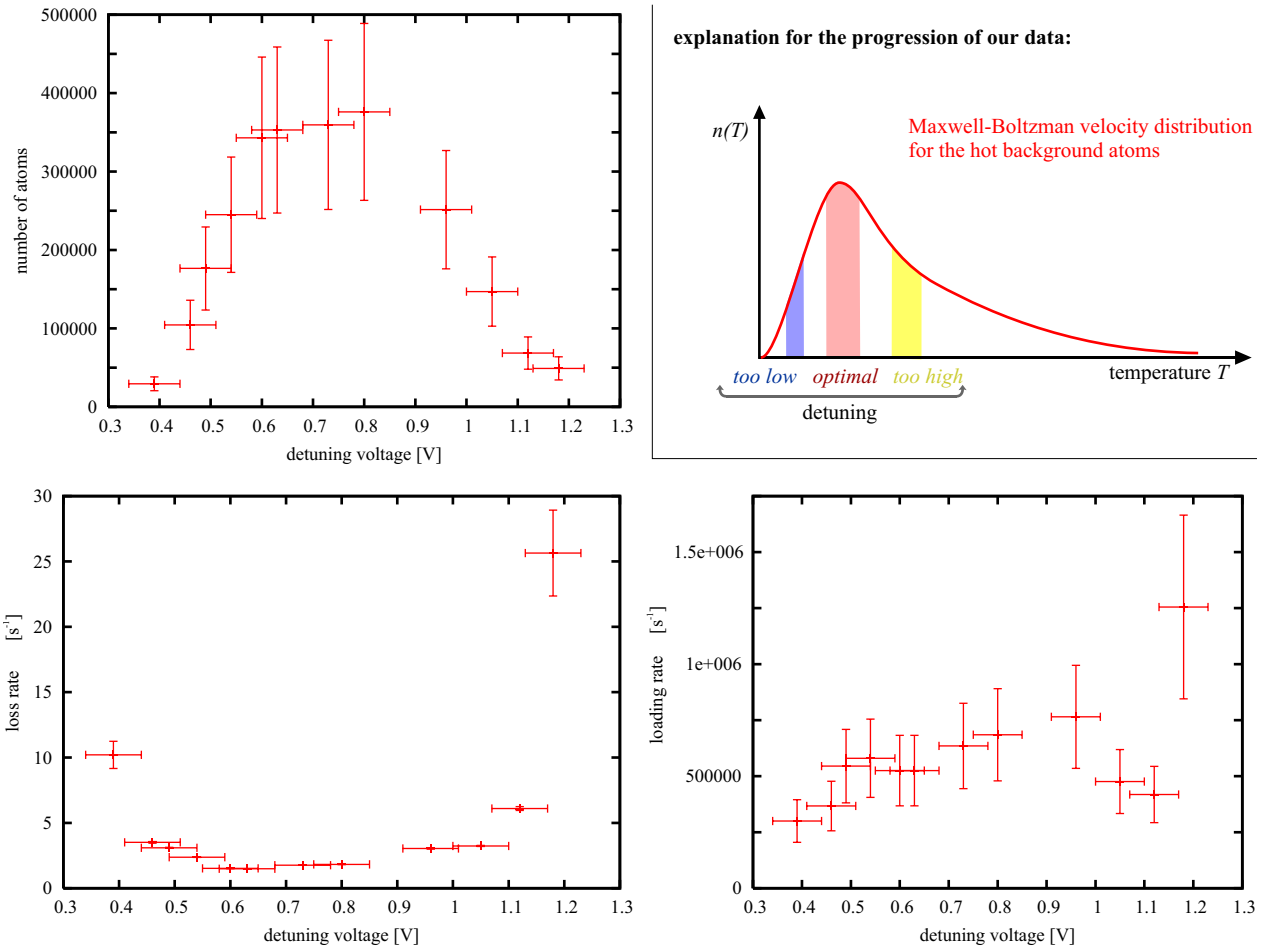

Figure 14: number of atoms N, loading rate γ and loss rate β versus detuning of the cooling laser

In all our further measurements we used a detuning of $U_{\text{detuning}} \approx 0.7\,\text{V}$ and a magnetic field current of $I_{\text{mag}} = 8..9\,\text{A}$.

We also tried to measure the conversion factor from the detuning voltage U_{detuning} to frequency shift $\Delta\nu$. To do this we measured the shift of one hyperfine line while changing U_{detuning}, using an oscilloscope. We did two series of measurements and got two different slopes for the linear fits. We could not explain this effect and did not have time to do more measurements, so we assumed that our calibration factor lies somewhere in between. Fig.15 shows our results. When assuming a slope halfway between the two measurements and a typical detuning voltage of $U_{\text{detuning}} = 0.7\,\text{V}$ we get a detuning in frequency of $\Delta\nu = (137 \pm 7)\,\text{MHz}$.

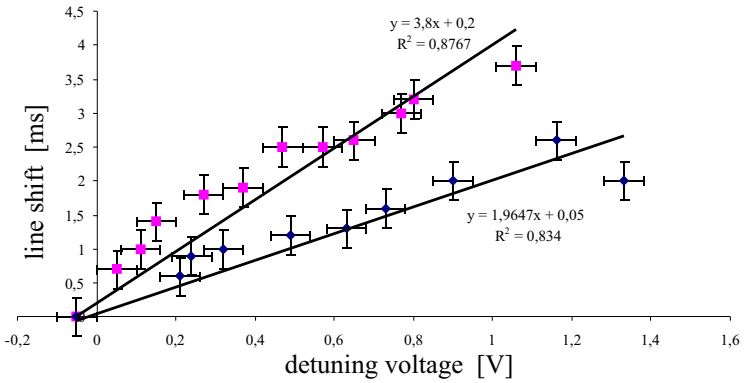

Figure 15: calibration of detuning versus detuning voltage

6.4 Temperature Measurements

6.4.1 Release and Recapture and a Naive Model

To get an estimate for the temperature of the trapped atoms, we used the so called release and recapture method. When the MOT is fully loaded one disrupts the laser for a short period of time (release time $\Delta t \approx 8..50$ ms). If this happens the atoms do no longer see the trap, so the cloud will expand ballistically. When the trap is back, only a fraction N_1/N_0 of the atomic cloud is recaptured.

If we assume that the velocities of the atoms are distributed according to a Maxwell-Boltzmann distribution, we can use this fraction to calculate the temperature. A naive model assumes that the atomic cloud's density is uniform over a sphere with radius σ_0. If the atoms move with the most probable velocity $v_p(T) = \sqrt{\frac{2k_BT}{m}}$ from the Maxwell-Boltzmann distribution, the radius of our sphere would increase with this velocity. So $\sigma_1 = \sigma_0 + v_p \cdot \Delta t$. From this one can get an expression for the temperature T and the ratio N_1/N_0:

$$T = \frac{m}{2k_B} \cdot \left[\frac{\sigma_0}{\Delta t} \cdot \left(\sqrt[3]{\frac{N_0}{N_1}} - 1 \right) \right]^2 \quad \Leftrightarrow \quad \frac{N_1}{N_0} = \left(1 + \frac{\Delta T}{\sigma_0} \cdot \sqrt{\frac{2k_BT}{m}} \right)^{-3} \tag{21}$$

Using this formula we estimated a temperature of about $T = (613 \pm 394)\ \mu$K ($U_{\text{detuning}} = 0.7$ V, $I_{\text{magn}} = 8.6$ A). The error is estimated by the standard deviation of about 12 measurements, T is their mean value. The Doppler limits for Rb is $T_{\text{Doppler}} \approx 140\ \mu$K. As the MOT in this lab is rather simple and does nut utilize sofisticated cooling methods the calculated temperature seems much too low.

6.4.2 Gaussian Model

We tried to construct a second model that should give estimates that are more realistic. To do this we assumes that the atoms have a Gaussian distribution in space. This is a better estimate, as an ideally harmonic potential would lead to such a distribution. If $n(\vec{x})$ is the particle density one would get the number of atoms by integrating over n:

$$N_{\text{trap}} = \iiint\limits_{V_{\text{trap}}} n(\vec{x}) d^3\vec{x} \qquad \text{with:} \quad n(\vec{x};\sigma) = n_0 \cdot \frac{1}{\sqrt{(2\pi\sigma)^3}} \cdot \exp\left\{ -\frac{\vec{x}^2}{2\sigma^2} \right\}$$

We can then assume that the radius that is defined by the standard deviation σ of the Gaussian distribution increases with velocity v_p, as above, so $\sigma(t = \Delta t) = \sigma(t = 0) + v_p \cdot \Delta t$. We can then calculate the fraction N_1/N_0 of atoms that are still inside the trap after the release time Δt:

$$\frac{N_1}{N_0}(\Delta t, T) = \frac{\int_0^{\sigma_0} n(\vec{x}; \sigma(T))\, d^3\vec{x}}{\int_0^{\sigma_0} n(\vec{x}; \sigma_0)\, d^3\vec{x}} \tag{22}$$

The integration can be done numerically, using Mathematica. Fig.16 shows the fraction N_1/N_0, in dependence of the temperature T for the naive and the Gaussian model.

For this plot we formulated the naive method from 6.4.1 in terms of integrals over propability distributions. We then get a distribution of the form:

$$n(\vec{x}; \sigma) = n_0 \cdot \begin{cases} \frac{3}{4\pi a^3} & |\vec{x}| \le a \\ 0 & |\vec{x}| > a \end{cases},$$

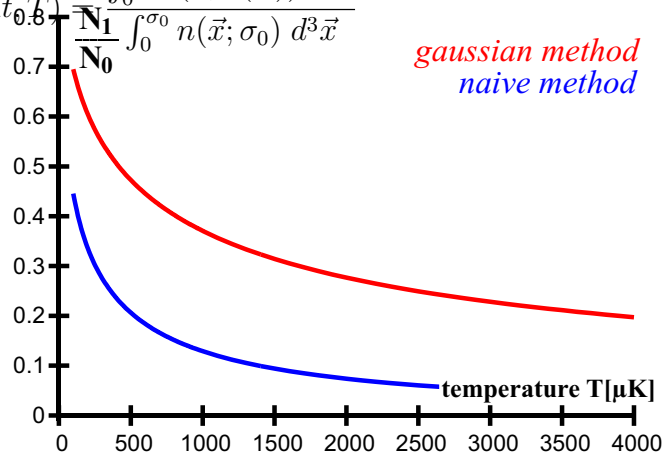

Figure 16: comparison between the results of a naive method, the Gaussian method for $\Delta t = 10$ ms with: $a = \sqrt{\frac{5}{3}} \cdot \sigma$

where a is the width of a uniform distribution with standard-deviation σ which models the atomic cloud. To compare these models we need to compare distributions with equal standard deviations.

6.4.3 Simulational Approach

There are still two important approximations in this Gaussian model, that do not have to be true. On the one hand we assume that the standard deviation (i.e. the typical radius of the trap) increases with $v_p(T)$. On the other hand this model neglects the gravitation. For the latter case we can make a short estimation. According to the theorem of centre of mass the cloud will fall down like a single particle that lies in it's centre of mass. Within a release time Δt the centre of mass moves then ($g = 9.81\ \frac{\mathrm{m}}{\mathrm{s}^2}$):

$$\Delta x = \frac{1}{2} g \cdot \Delta t^2 \approx \begin{cases} 0.5\ \mathrm{mm} & \text{for } \Delta t = 10\ \mathrm{ms} \\ 2\ \mathrm{mm} & \text{for } \Delta t = 20\ \mathrm{ms} \end{cases}$$

As this length is in the same order of magnitude as the diameter of the atomic cloud it may not be neglected, as it leads to a measurable loss during the experiment. To find a model that accounts for this also, we wrote a computer program, that simulates the expansion of the cloud. For this simulation we assume that the atoms have a Gaussian distribution in space with the same size in all directions (i.e. a spherical ball). The absolute values of the velocities were distributed according to the Maxwell-Boltzman distribution and their directions are uniformly distributed in space. We then let the cloud expand, i.e. we calculate:

$$\vec{x}_i(\Delta t) = \vec{x}_i + \vec{v}_i \cdot \Delta t - \frac{1}{2} \begin{pmatrix} 0 \\ 0 \\ g \end{pmatrix} \cdot \Delta t^2. \tag{23}$$

The third part of (23) calculates the effect of gravity in z-direction. Before and after this expansion step, we count all atoms that satisfy $|\vec{x}_i| \le \sigma_0$. From the two counting steps we can compute N_1/N_0. As we start with randomly distributed atoms. Listing 1 summarises these steps.

6.4.4 Comparison of the models

Fig.17 shows a comparison between all three methods. As one can see the curves have in about the same shape, but they predict very different temperatures. $N_1/N_0 = 20\%$ is a typical

Algorithm 1 ballistic expansion of atomic cloud

for all $T_{\min} \leq T \leq T_{\max}$ **do**
  create N_{start} randomly distributed atoms
  $N_0 \leftarrow$ (number of atoms i with $|\vec{x}_i| \leq \sigma_0$) ▷ count atoms in trap
  for all atoms i **do**
    $\vec{x}_i(\Delta t) = \vec{x}_i + \vec{v}_i \cdot \Delta t - \frac{1}{2}\begin{pmatrix}0\\0\\g\end{pmatrix} \cdot \Delta t^2$ ▷ propagate all atoms
  end for
  $N_1 \leftarrow$ (number of atoms i with $|\vec{x}_i| \leq \sigma_0$) ▷ count atoms in trap
  output N_1/N_0
end for

loss rate for the parameters in this simulation ($\Delta t = 10$ ms), which was extracted from the experiment. With this loss rate we would predict these temperatures:

$$T_{\text{naive}} = 530\ \mu\text{K}; \qquad T_{\text{gauss}} = 4\ \text{mK}; \qquad T_{\text{simulation}} = 2.95\ \text{mK}$$

For small release times gravity does not have a major effect on the value of N_1/N_0. If the release time is longer $\Delta t \approx 20$ ms one can observe a slightly smaller values for N_1/N_0 ($\Delta N/N \approx 0.5..1\%$), if the temperature is low. For higher temperatures the velocity of the atoms is much larger than the additional velocity by gravitational acceleration and the effect can again be neglected. For the range of N_1/N_0 in our experiment the gaussian model and the simulation give temperatures that are in about same order of magnitude whereas the naive model gives temperatures that are about one order of magnitude lower.

Without a further temperature measurement using another, independent method (e.g. observe expansion with a CCD camera) we cannot determine which model is valid for our experiment, but we believe that the naive model is too unrealistic to give good results. We also do not completely understand the results of our simulation, especially the behaviour for higher temperatures.

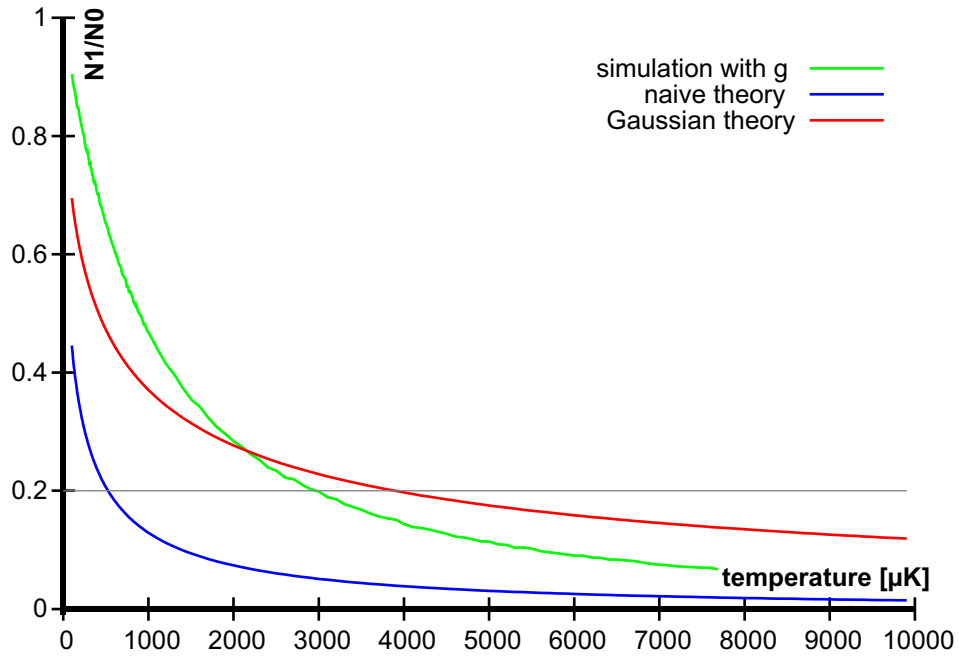

Figure 17: comparison between the naive model, the Gaussian model and our simulation. (parameters: $\Delta t = 10$ ms; $N_{\text{start}} = 500000$; $\sigma_0 = 3.5$ mm)

7 Appendix

7.1 physical constants and data

Boltzman-constant:	$k_B = 1.3807 \cdot 10^{23}$ J/K
mass of ^{85}Rb:	$m_{Rb85} = \frac{85\,\mathrm{g/mol}}{6.022 \cdot 10^{23}\,\mathrm{mol}^{-1}} = 1.411 \cdot 10^{-25}$ kg
mass of ^{87}Rb:	$m_{Rb87} = \frac{87\,\mathrm{g/mol}}{6.022 \cdot 10^{23}\,\mathrm{mol}^{-1}} = 1.445 \cdot 10^{-25}$ kg
central wavelength of Rb D2-line:	$\lambda_{D2} = 780.027$ nm
decay rate of the excited Rb-D_2 state:	$\Gamma_{\mathrm{D2}} = 3.77 \cdot 10^7\ \mathrm{s}^{-1}$

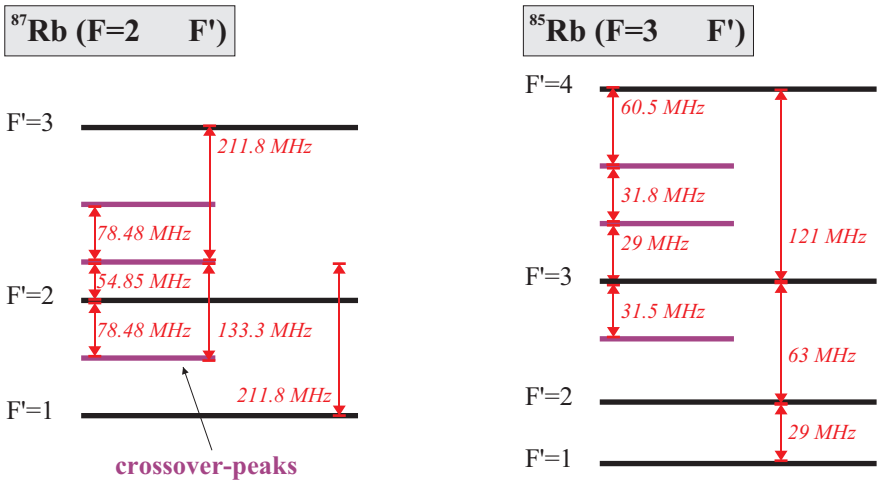

Figure 18: part of the theoretical hyperfine spectrum of Rb D_2-line

References

[Demtröder 2002] *Demtröder, Wolfgang (2002):* **Experimentalphysik 3. Atome, Moleküle und Festkörper**, 2. Auflage, New York - Berlin - Heidelberg: Springer Verlag.

[Haken 2000] *Haken, Herrman Wolf, Hans Christoph:* **"Atom- und Quantenphysik"**, 7. Auflage, Berlin - Heidelberg - New York: Springer Verlag.

[Kemmann 2001] *Kemmann, Mark (2001):* **Laserinduzierte und spontane Molekülbildung in einer magneto-optischen Atomfalle.** Albert-Ludwigs-Universität Freiburg im Breisgau: diploma thesis. [http://frhewww.physik.uni-freiburg.de/photoa/dipl.pdf]

[Mot 2004] Versuchsanleitung F20, Magnetooptische Falle

[Phillips 1992] *Phllips, W.D.:* **"Laser cooling and trapping of neutral atoms", in Laser Manipulation of Atoms and Ions**, Proc. Enrico Fermi Summer School, Course CXVIII, Varenna, Italy, July, 1991, edited by E. Arimondo, W.D. Phillips, and F. Strumia (North-Holland, Amsterdam, 1992)

[Steck 2005] *Steck, Daniel (2005):* **Alkali D Line Data.** accessed: 20.04.2005 (URL: http://george.ph.utexas.edu/~dsteck/alkalidata/)

[Stuhler 2001] *Stuhler, Jürgen (2001):* **Kontinuierliches Laden einer Magnetfalle mit lasergekühlten Chromatomen.** univerity of Konstanz: PhD thesis. [http://www.ub.uni-konstanz.de/v13/volltexte/2001/726//pdf/stuhler.pdf]